COMMUNICATION

Check for updates

Direct photopatterning and erasing of quantum dots *via* ligand photoisomerization

Zhong Fu,†[a] Zhi Zheng,†[a] Yu Xie,†[b] Hannikezi Abudukeremu,[a] Likuan Zhou,[c] Shuangan Zang,[b] Kunfei Tian,[c] Qiuyu Liu,[c] Yuan Li[b] and Hao Zhang [ID] *[a]

We report direct photopatterning and erasing of colloidal quantum dots (QDs) *via* a ligand photoisomerization mechanism. Unlike previous approaches involving bond formation or breaking, the reversible ligand isomerization under UV and visible light modulates colloidal solubility, enabling high-fidelity writing and "on-demand" erasure of QD patterns while maintaining their luminescent properties.

Colloidal semiconductor nanocrystals, especially colloidal quantum dots (QDs) with sizes within the quantum confinement regime, have emerged as important candidates for a wide range of optoelectronic, electronic, and quantum devices.[1–6] Over the past few decades, deepened understanding of the QD–surface ligand interactions has stimulated the development of QDs with rationally engineered photophysical properties, as well as devices whose performance rivals that of bulk semiconductors.[7–12] These advances enable their applications as color-conversion layers in commercial QD televisions and pave the way for further developments in electroluminescent (EL) QD light-emitting diode (QLED) displays.[13–16]

Despite significant material and device advances, integrated systems such as displays and image sensors still require patterning strategies that position QD layers with high spatial precision while preserving functionality.[17–19] Among existing approaches, resist-free direct photopatterning is particularly attractive due to its compatibility with colloidal materials and ability to deliver high resolution and fidelity.[19–22] This method, as exemplified in the DOLFIN approach by Talapin and co-workers,[23,24] is also based on the QD–surface ligand

interactions. Under light stimulation, the photochemical changes in the ligands or QD surface induce large changes in QD colloidal solubility. The light-induced colloidal solubility contrast then enables selective dissolution/removal of QDs in exposed/unexposed regions, forming QD films with desirable patterns. Recent efforts in direct photopatterning[25–36] have enabled large-scale (6-inch wafers), full-color patterning of QDs with resolution over 10 000 pixels per inch (smallest feature size <1 μm), as well as proof-of-concept patterned QLEDs with external quantum efficiency (EQEs) of ∼20%, approaching the state-of-the-art non-patterned QLEDs. However, we note that all existing ligand photochemistries for direct photopatterning of QDs involve the formation (*e.g.*, ligand photocrosslinking,[25,26,29,32,34,37–41] ligand binding[42,43]) or the breaking (*e.g.*, ligand decomposition,[23,24,44] ligand desorption/exchange[30,33,45]) of chemical bonds in the ligands or QD–ligand interfaces. This raises the question of whether dynamic (instead of permanent) ligand photochemistries can support direct photopatterning of QDs and introduce more functionalities.

Here, we report a new mechanism for direct photopatterning of QDs, which does not involve permanent, photoinduced bond formation or breaking. This method exploits a photosensitive ligand with an azobenzene group (or AZO ligands, for short), whose photoisomerization between *trans* and *cis* states reversibly tunes the interparticle dipole–dipole interaction and colloidal solubility of QDs. Specifically, QDs with dual ligands (native ligands and AZO ligands) become insoluble upon 365-nm UV irradiation and recover their colloidal stability after visible light (450 nm) illumination. The former process enables direct, multicolored photopatterning of various QDs with high resolution (∼2 μm) and other patterning capabilities on par with existing methods. The latter process, where the AZO ligands return to the *trans* state, enables the "on-demand" erasure of QD layers. We also investigated the photoluminescent (PL) and EL properties of patterned QDs. The wavelength-dependent direct photopatterning ("writing") and "erasing" of pixelated QD layers may enable applications in optical information encryption, selective replacement of components in

[a] *Department of Chemistry, Center for BioAnalytical Chemistry, Key Laboratory of Bioorganic Phosphorus Chemistry & Chemical Biology (Ministry of Education), Tsinghua University, Beijing 100084, China.*
  E-mail: hzhangchem@mail.tsinghua.edu.cn

[b] *Department of Chemistry, Key Laboratory of Organic Optoelectronics & Molecular Engineering (Ministry of Education), Tsinghua University, Beijing 100084, China*

[c] *National Center of Technology Innovation for Display, Guangzhou, Guangdong 510525, China*

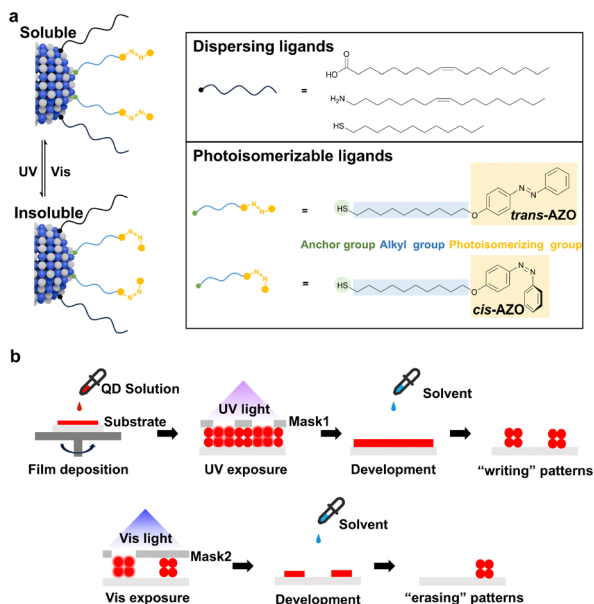† Z. Fu, Z. Zheng and Y. Xie contributed equally to this work.

Fig. 1 Scheme of the photoisomerization based direct photopatterning and erasing of QDs with dual ligands. (a) Schematic illustration of the reversible, photoisomerization-mediated modulation of colloidal stability in dual-ligand capped QDs. (b) Process flow of wavelength-dependent direct photopatterning ("writing") and erasure of QD films.

integrated devices, and other functionalities inaccessible to photopatterning schemes based on permanent ligand formation or breaking.

The patterning mechanism is inspired by the reversible light-controlled assembly of azobenzene-functionalized gold nanoparticles.[46–48] Unlike these fundamental assembly studies, our work targets high-resolution photopatterning for functional optoelectronics. Specifically, we functionalized the QDs with dual ligands. The native oleic acid (OA), oleylamine (OLA) or 1-dodecanethiol (DDT) ligands were introduced during QD synthesis, providing surface passivation and colloidal dispersibility. These dispersing ligands were partially exchanged post-synthetically with the photoisomerizable AZO ligands, which contain a thiol group for binding to the QD surface and an azobenzene group responsible for photoisomerization and patterning (Fig. 1a). Information on synthesis and characterization of the AZO ligand appears in Fig. S1–S4. The resultant dual-ligand capped QDs, with the AZO ligands in the *trans* state, disperse well in nonpolar solvents such as toluene. Upon UV irradiation (*e.g.*, 365 nm), the AZO group on the ligands undergoes rapid *trans*-to-*cis* photoisomerization, accompanied with a significant increase in dipole moment.[47,49] The enhanced dipole–dipole interaction between AZO ligands in the *cis* state contributes to a non-negligible adhesion energy between two adjacent QDs ($\sim 3.5\ k_{\rm B}$T), which is larger than the thermal energy ($1.5 k_{\rm B}$T).[46] Such additional adhesion energy disrupts the balance between the attractive van der Waals ($\Phi_{\rm vdW}$) and repulsive osmotic interactions ($\Phi_{\rm osm}$) of QDs, driving their aggregation (Fig. S5).

Conversely, exposing the unstable colloids to visible light (*e.g.*, 405 or 450 nm) induces *cis*-to-*trans* back-isomerization,

restoring the colloidal stability of the QDs. The reversible colloidal stability changes enable the wavelength-dependent, direct photo-patterning (or writing) and erasure of QD films. Fig. 1b depicts the patterning and erasing procedures: (i) solution-based coating of QD films with dual ligands; (ii) selective UV exposure (365 nm) *via* photomasks to induce *trans*-to-*cis* isomerization of AZO ligands on QDs in the exposed regions; (iii) development by nonpolar solvent to remove QDs in unexposed regions to form patterns. For erasure, the formed QD patterns can be treated by (iv) selective visible-light (405 or 450 nm) exposure to cause *cis*-to-*trans* isomerization in the AZO ligands, restoring the colloidal stability of QDs in nonpolar solvents and (v) enabling targeted removal of QDs in irradiated areas.

We performed spectroscopic analyses to elucidate the photo-chemical processes underlying QD patterning and erasure. The wavelength-dependent reversible switching of AZO ligands between *trans* and *cis* states underpins the isomerization-based mechanism. As shown in Fig. S6, AZO ligands in toluene solution exhibit two characteristic absorption bands: a strong π–π^* transition band (centered at $\sim$ 350 nm) and a weaker n–π^* transition band (centered at $\sim$450 nm). Under 365 nm UV irradiation, we observed a gradual decrease of the π–π^* transition intensity (corresponding to the *trans* isomer) with the increase of the n–π^* transition (*cis* isomer). This *trans*-to-*cis* photoisomerization efficiency can reach $> 90\%$ with a UV dose of 100 mJ cm^{-2}. The reverse *cis*-to-*trans* conversion is also efficient under 450 nm irradiation, as evidenced by the complete recovery of absorption features of the *trans*-isomers.

Second, the AZO ligands readily bind to the QD surface and partially replace native organic ligands through a solution-phase ligand-exchange process (SI). The ligand exchange process was efficient and required about 1 h to bind sufficient AZO ligands for achieving satisfactory patterning quality (Fig. S7). We used red-emitting CdSe-based QDs with native OA ligands (diameter $\approx$ 13 nm, transmission electron microscopic image and optical spectra shown in Fig. S8) as a model system. After ligand exchange, the QDs preserved their sizes and colloidal dispersity (Fig. S9). Fourier-transform infrared (FTIR) spectra (Fig. S10) confirmed the successful anchoring of AZO ligands. A combination of thermogravimetric, proton nuclear magnetic resonance (^{1}H-NMR) analysis (Fig. S11), and associated calculations (SI) provided a quantitative evaluation of the numbers/percentage of OA (923 ligands, 52%) and AZO ligands (876 ligands, 48%) per QD. The *cis*-AZO dipoles can generate an interparticle attraction of approximately 2.1 kcal mol^{-1} (or $3.5 k_{\rm B}$T, see calculations in the SI), which is sufficient to induce QD aggregation after 365 nm UV exposure. Moreover, the AZO ligands retain their photoisomerization capabilities when functionalized on the QD surface (Fig. S12). Such reversible configurational changes constitute a new type of direct patterning method for QDs, complementing those involving irreversible bond formation or breaking.

Fig. 2 shows the images of patterned QD layers with dual-ligands. Because the patterning relies solely on the *trans*-to-*cis* configurational changes of the AZO ligands, this method is applicable to different types of colloidal QDs, including CdSe-,
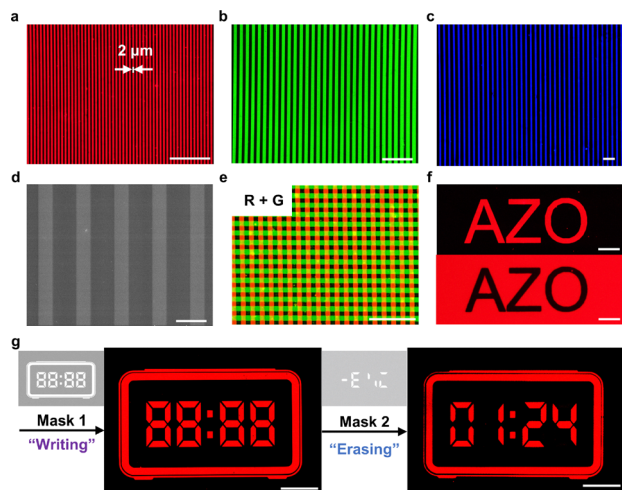
Fig. 2 Reconfigurable direct photopatterning of QD films. (a)–(c) Optical micrographs of patterned RGB QD films generated *via* selective 365 nm UV exposure, achieving a minimum feature size of 2 μm. (d) Top-view SEM image of representative patterned QD stripes. (e) Sequential photopatterning of red and green QDs. (f) Positive (top) and negative (bottom) QD patterns produced through UV "writing" (365 nm) and visible-light "erasing" (405 nm) steps, respectively, using the same mask. (g) Two-step "write–erase" demonstration. Scale bars, (a)–(d) 50 μm; (e) 500 μm; (f and g) 100 μm.

and InP-based materials (Fig. S13 and S14). These patterns were typically made with UV (365 nm) doses in the range of 300–600 mJ cm^{-2}. Fig. 2a–c shows the finest feature size of about 2 μm, replicating that of the pre-designed photomasks. The quality of these patterned QD layers was further characterized by atomic force microscopy (AFM) and scanning electron microscopy (SEM) images. The patterned QD layers maintained their original surface roughness (~2 nm) and film morphology after patterning (Fig. S15 and S16). The patterned QD layers showed high film quality and sharp edges, as confirmed by top-view SEM images and height profile analysis (Fig. 2d and Fig. S17). Regardless of the reversible nature, the metastable *cis* state of the AZO ligands can remain for a relatively long time (hours to days under ambient conditions[47]). This allows us to perform consecutive patterning of multiple layers. Fig. 2e and Fig. S18 show the patterns obtained by sequential patterning of QDs with different emitting colors, where the subsequent layer patterning does not affect the underlying layers. Notably, the physical pattern remains fixed even after back-isomerization, as "erasure" requires a solvent developer.

The reversible photoisomerization-based mechanism further enables the "on demand" erasure of QD layers under visible light illumination. For example, the same photomask can be used to generate both positive and negative patterns. In Fig. 2f, the upper image shows the positive pattern made with the "AZO" photomask under 365 nm UV light illumination, as described above. The bottom negative image was obtained by a flood exposure (namely, exposing the entire QD film) under 365 nm light, and then the selective exposure to 405 nm light *via* the same photomask. The visible light irradiation triggered the *cis*-to-*trans* back-conversion of the AZO ligands, making the exposed QDs dispersible in toluene for the erasure. Typical exposure parameters for

making such negative patterns include flood exposure at 365 nm for 300 mJ cm^{-2} and selective exposure at 405 nm for 500 mJ cm^{-2}. Using similar procedures, we can also firstly "write" a pattern on QD films using 365 nm UV light and then "erase" selected regions using 405 nm visible light. As shown in Fig. 2g, the initial UV-induced writing step (365 nm, Mask 1) generates a complete digital-clock pattern displaying "88 : 88". A subsequent visible-light exposure (405 nm, Mask 2) selectively removes designated segments, converting the intermediate "88 : 88" display into a new, user-defined time display of "01 : 24". We also made a demonstration using a Tetris-style pattern (Fig. S19). These two examples highlight the ability of our wavelength-dependent process to reconfigure complex patterns on demand, enabling applications such as dynamic displays, reprogrammable micro-patterns, and information encryption with spatial and spectral selectivity.[50,51]

We then evaluated the effect of this photoisomerization method on the PL and EL properties of the QDs. In principle, the photochemistry of this method involves only the photoisomerization of AZO ligands, which avoids the critical issues of ligand detachment, active radical formation, and side reactions that may introduce surface defects or performance degradation during patterning. Fig. 3a shows the PL emission spectra of patterned QD films, which remain identical to the OA-capped QD films. Fig. 3b compares the changes in the photoluminescence quantum yields (PLQYs) of red-emitting core–shell QDs at various stages of patterning in air, including pristine QDs (with OA ligands), after ligand exchange (with dual-ligands), after UV exposure (365 nm), after development with toluene, and after visible-light exposure (to mimic erasing condition). As revealed by surface ligand analysis in Fig. S11, the ligand-exchange process maintained consistent ligand density (~3 nm^{-2}, see discussions in the SI), indicating that no additional surface defects were introduced. The patterned red QD films retained ~92% of the initial PLQYs for pristine QDs. We also measured the PLQYs of green QDs (Fig. S20 and Table S1). A PLQY reduction was observed, primarily due to hole transfer driven by energy level alignment after ligand exchange (Fig. S21). This quenching could be avoided by designing new AZO ligands with lowered HOMO levels through electron-withdrawing substituents or heteroaromatic rings.[52] The PLQY trends corroborate the PL decay behaviour of the corresponding samples during patterning (Fig. S22). Moreover, repeated structural switching between *trans* and *cis* states for 5 cycles caused no PLQY degradation (Fig. S23).

Finally, we fabricated QLED devices using dual-ligand capped, red CdZnSe/CdZnS/ZnS QDs as the emissive layer. Fig. 3c illustrates the device structure of QLEDs and Fig. S24 shows the energy levels of functional layers. For evaluating the effect of the patterning procedures on the EL properties, we compared the performance of pristine and patterned devices, whose QD emission layer was prepared under different conditions, as described in the SI. Both types of devices exhibited comparable EL characteristics, as shown in Fig. 3d–f and Fig. S25. Nearly identical current density–voltage–luminance (J–V–L) characteristics and EQE curves confirmed that the isomerization of the AZO ligand did not compromise the EL
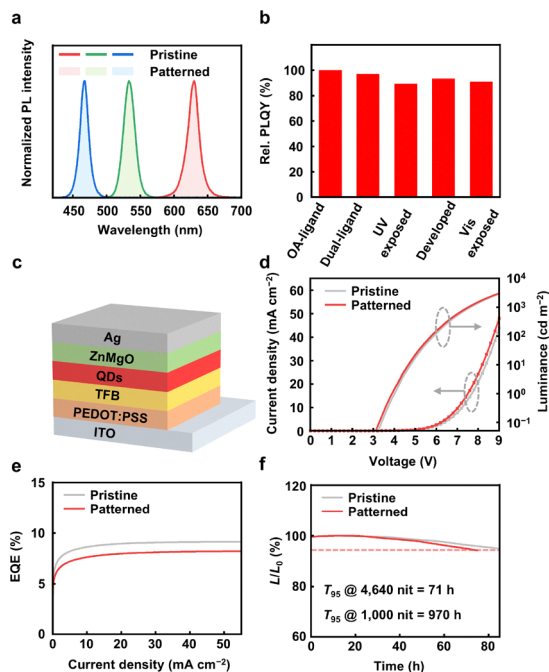
Fig. 3 PL and EL characterization of QDs during photopatterning and erasure. (a) Normalized PL emission spectra of pristine and patterned QD films. (b) Relative PLQYs of red QDs at different processing stages. (c) Schematic of the QLED structure. (d)–(f) J–V–L characteristics, EQE, and lifetime of the pristine and patterned QLEDs.

performance of the QDs. The patterned devices showed a low turn-on voltage of 3.0 V and a peak EQE of 8.2%. The operation lifetime of the patterned QLEDs (extrapolated T_{95} at 1000 cd m^{-2}, 970 h) is comparable to that of the pristine devices (1120 h). Furthermore, the EL performance of devices during the *trans–cis–trans* switching of the AZO ligands remained largely unchanged (Fig. S26).

In conclusion, we have introduced a reversible photopatterning strategy for colloidal QDs based on *trans–cis* isomerization of surface-anchored AZO ligands. Unlike conventional approaches that rely on irreversible photochemical bond formation or breaking events, this method enables wavelength-selective "writing" and "erasing" of QD patterns without permanent chemical changes. These features make the strategy promising for adaptive optoelectronic architectures, rewritable optical elements, and information encryption/decryption.

Conflicts of interest

There are no conflicts to declare.

Data availability

The data supporting this article have been included as part of the supplementary information (SI). Supplementary information is available. See DOI: https://doi.org/10.1039/d5cc07216f

Acknowledgements

References

1 M. V. Kovalenko, L. Manna, A. Cabot, Z. Hens, D. V. Talapin, C. R. Kagan, V. I. Klimov, A. L. Rogach, P. Reiss, D. J. Milliron, P. Guyot-Sionnnest, G. Konstantatos, W. J. Parak, T. Hyeon, B. A. Korgel, C. B. Murray and W. Heiss, *ACS Nano*, 2015, **9**, 1012–1057.
2 A. L. Efros and L. E. Brus, *ACS Nano*, 2021, **15**, 6192–6210.
3 C. R. Kagan, E. Lifshitz, E. H. Sargent and D. V. Talapin, *Science*, 2016, **353**, aac5523.
4 F. P. García De Arquer, D. V. Talapin, V. I. Klimov, Y. Arakawa, M. Bayer and E. H. Sargent, *Science*, 2021, **373**, eaaz8541.
5 C. R. Kagan, L. C. Bassett, C. B. Murray and S. M. Thompson, *Chem. Rev.*, 2021, **121**, 3186–3233.
6 C. R. Kagan, *Chem. Soc. Rev.*, 2019, **48**, 1626–1641.
7 J. Owen and L. Brus, *J. Am. Chem. Soc.*, 2017, **139**, 10939–10943.
8 M. A. Boles, D. Ling, T. Hyeon and D. V. Talapin, *Nat. Mater.*, 2016, **15**, 141–153.
9 Y.-S. Park, J. Roh, B. T. Diroll, R. D. Schaller and V. I. Klimov, *Nat. Rev. Mater.*, 2021, **6**, 382–401.
10 Y. Shirasaki, G. J. Supran, M. G. Bawendi and V. Bulović, *Nat. Photonics*, 2013, **7**, 13–23.
11 C. R. Kagan and C. B. Murray, *Nat. Nanotechnol.*, 2015, **10**, 1013–1026.
12 M. Ibáñez, S. C. Boehme, R. Buonsanti, J. De Roo, D. J. Milliron, S. Ithurria, A. L. Rogach, A. Cabot, M. Yarema, B. M. Cossairt, P. Reiss, D. V. Talapin, L. Protesescu, Z. Hens, I. Infante, M. I. Bodnarchuk, X. Ye, Y. Wang, H. Zhang, E. Lhuillier, V. I. Klimov, H. Utzat, G. Rainò, C. R. Kagan, M. Cargnello, J. S. Son and M. V. Kovalenko, *ACS Nano*, 2025, **19**, 31969–32051.
13 X. Dai, Z. Zhang, Y. Jin, Y. Niu, H. Cao, X. Liang, L. Chen, J. Wang and X. Peng, *Nature*, 2014, **515**, 96–99.
14 Y.-H. Won, O. Cho, T. Kim, D.-Y. Chung, T. Kim, H. Chung, H. Jang, J. Lee, D. Kim and E. Jang, *Nature*, 2019, **575**, 634–638.
15 T. Kim, K.-H. Kim, S. Kim, S.-M. Choi, J. Hang, H.-K. Seo, H. Lee, D.-Y. Chung and E. Jang, *Nature*, 2020, **586**, 385–389.
16 Y. Bian, X. Yan, F. Chen, Q. Li, B. Li, W. Hou, Z. Lu, S. Wang, H. Zhang, W. Zhang, D. Zhang, A. Tang, F. Fan and H. Shen, *Nature*, 2024, **635**, 854–859.
17 J. Yang, M. K. Choi, U. J. Yang, S. Y. Kim, Y. S. Kim, J. H. Kim, D.-H. Kim and T. Hyeon, *Nano Lett.*, 2021, **21**, 26–33.
18 S. Baek and J. S. Son, *Adv. Phys. Res.*, 2024, **3**, 2300069.
19 S. Y. Park, S. Lee, J. Yang and M. S. Kang, *Adv. Mater.*, 2023, **35**, 2300546.
20 S. Maeng and H. Cho, *Acc. Mater. Res.*, 2025, **6**, 393–398.
21 Y. Yang, J. Guan, N. Zhang, L. Ru, Y. Zou and Y. Wang, *J. Mater. Chem. A*, 2024, **12**, 32505–32525.
22 J.-A. Pan, H. Cho, I. Coropceanu, H. Wu and D. V. Talapin, *Acc. Chem. Res.*, 2023, **56**, 2286–2297.
23 Y. Wang, I. Fedin, H. Zhang and D. V. Talapin, *Science*, 2017, **357**, 385–388.
24 Y. Wang, J.-A. Pan, H. Wu and D. V. Talapin, *ACS Nano*, 2019, **13**, 13917–13931.
25 J. Yang, D. Hahm, K. Kim, S. Rhee, M. Lee, S. Kim, J. H. Chang, H. W. Park, J. Lim, M. Lee, H. Kim, J. Bang, H. Ahn, J. H. Cho, J. Kwak, B. Kim, C. Lee, W. K. Bae and M. S. Kang, *Nat. Commun.*, 2020, **11**, 2874.
26 D. Hahm, J. Lim, H. Kim, J.-W. Shin, S. Hwang, S. Rhee, J. H. Chang, J. Yang, C. H. Lim, H. Jo, B. Choi, N. S. Cho, Y.-S. Park, D. C. Lee, E. Hwang, S. Chung, C. Kang, M. S. Kang and W. K. Bae, *Nat. Nanotechnol.*, 2022, **17**, 952–958.
27 J. Yang, M. Lee, S. Y. Park, M. Park, J. Kim, N. Sitapure, D. Hahm, S. Rhee, D. Lee, H. Jo, Y. H. Jo, J. Lim, J. Kim, T. J. Shin, D. C. Lee, K. Kwak, J. S. Kwon, B. Kim, W. K. Bae and M. S. Kang, *Adv. Mater.*, 2022, **34**, 2205504.

28 D. Liu, K. Weng, S. Lu, F. Li, H. Abudukeremu, L. Zhang, Y. Yang, J. Hou, H. Qiu, Z. Fu, X. Luo, L. Duan, Y. Zhang, H. Zhang and J. Li, *Sci. Adv.*, 2022, **8**, eabm8433.

29 S. Lu, Z. Fu, F. Li, K. Weng, L. Zhou, L. Zhang, Y. Yang, H. Qiu, D. Liu, W. Qing, H. Ding, X. Sheng, M. Chen, X. Tang, L. Duan, W. Liu, L. Wu, Y. Yang, H. Zhang and J. Li, *Angew. Chem., Int. Ed.*, 2022, **61**, e202202633.

30 Z. Fu, L. Zhou, Y. Yin, K. Weng, F. Li, S. Lu, D. Liu, W. Liu, L. Wu, Y. Yang, H. Li, L. Duan, H. Xiao, H. Zhang and J. Li, *Nano Lett.*, 2023, **23**, 2000–2008.

31 F. Li, C. Chen, S. Lu, X. Chen, W. Liu, K. Weng, Z. Fu, D. Liu, L. Zhang, H. Abudukeremu, L. Lin, Y. Wang, M. Zhong, H. Zhang and J. Li, *ACS Nano*, 2022, **16**, 13674–13683.

32 Z. Fu, S. F. Musolino, W. Qing, H. Li, F. J. De Zwart, Z. Zheng, M. Cai, Y. Gao, B. De Bruin, X. Dai, J. E. Wulff and H. Zhang, *J. Am. Chem. Soc.*, 2024, **146**, 28895–28905.

33 H. Cho, J. Pan, H. Wu, X. Lan, I. Coropceanu, Y. Wang, W. Cho, E. A. Hill, J. S. Anderson and D. V. Talapin, *Adv. Mater.*, 2020, **32**, 2003805.

34 P. Xiao, J. Ma, Z. Zhang, Y. Zou, H. Luo, J. Guan, J. Zhang, L. Zhou, W. Hou, P. Zhang, D. V. Talapin and Y. Wang, *ACS Nano*, 2025, **19**, 14509–14520.

35 Q. Nie, J. Fan, R. Xu, Z. Yao, Y. Xiao, C. Xiang, L. Qian and T. Zhang, *Adv. Funct. Mater.*, 2025, 2420829.

36 N. Lee, D. Choi, K.-J. Ko, H.-S. Kim, J. H. Yu and J.-S. Lee, *ACS Nano*, 2025, **19**, 22253–22261.

37 D. Liu, K. Weng, H. Zhao, S. Wang, H. Qiu, X. Luo, S. Lu, L. Duan, S. Bai, H. Zhang and J. Li, *ACS Nano*, 2024, **18**, 6896–6907.

38 S. Maeng, S. J. Park, J. Lee, H. Lee, J. Choi, J. K. Kang and H. Cho, *Sci. Adv.*, 2023, **9**, eadi6950.

39 S. Maeng, J. Kim, T. Kim, S. Lee, S. Han, S. J. Park, C. Kim, J. Kim, J. Lee and H. Cho, *Adv. Mater.*, 2025, e08217.

40 P. Zhang, G. Yang, F. Li, J. Shi and H. Zhong, *Nat. Commun.*, 2022, **13**, 6713.

41 W. Qing, Y. Si, M. Cai, L. Zhou, L. Wu, Z. Hou, D. Liu, X. Tian, W. Liu, L. Lin and H. Zhang, *Nano Res.*, 2024, **17**, 10460–10466.

42 P. Xiao, Z. Zhang, J. Ge, Y. Deng, X. Chen, J.-R. Zhang, Z. Deng, Y. Kambe, D. V. Talapin and Y. Wang, *Nat. Commun.*, 2023, **14**, 49.

43 J.-A. Pan, H. Wu, A. Gomez, J. C. Ondry, J. Portner, W. Cho, A. Hinkle, D. Wang and D. V. Talapin, *ACS Nano*, 2022, **16**, 16067–16076.

44 J.-A. Pan, J. C. Ondry and D. V. Talapin, *Nano Lett.*, 2021, **21**, 7609–7616.

45 J. Lee, J. Ha, H. Lee, H. Cho, D. C. Lee, D. V. Talapin and H. Cho, *ACS Energy Lett.*, 2023, **8**, 4210–4217.

46 R. Klajn, K. J. M. Bishop and B. A. Grzybowski, *Proc. Natl. Acad. Sci. U. S. A.*, 2007, **104**, 10305–10309.

47 R. Klajn, P. J. Wesson, K. J. M. Bishop and B. A. Grzybowski, *Angew. Chem., Int. Ed.*, 2009, **48**, 7035–7039.

48 D. Manna, T. Udayabhaskararao, H. Zhao and R. Klajn, *Angew. Chem., Int. Ed.*, 2015, **54**, 12394–12397.

49 H. Akiyama, K. Tamada, J. Nagasawa, K. Abe and T. Tamaki, *J. Phys. Chem. B*, 2003, **107**, 130–135.

50 J. Hu, S. Zhu, M. Gu and Y. Zhang, *ACS Photonics*, 2024, **11**, 2007–2015.

51 H. Han, J. W. Oh, H. Lee, S. Lee, S. Mun, S. Jeon, D. Kim, J. Jang, W. Jiang, T. Kim, B. Jeong, J. Kim, D. Y. Ryu and C. Park, *Adv. Mater.*, 2024, **36**, 2310130.

52 S. Crespi, N. A. Simeth and B. König, *Nat. Rev. Chem.*, 2019, **3**, 133–146.